Journal of the European Ceramic Society 22 (2002) 2165–2171

www.elsevier.com/locate/jeurceramsoc

Toughening of alumina/zirconia ceramic composites with silver particles

Jérôme Lalande*,[1], Sven Scheppokat, Rolf Janssen, Nils Claussen

Arbeitsbereich Technische Keramik, Technische Universität Hamburg-Harburg, Denickestrasse 15, 21073 Hamburg, Germany

Received 1 August 2001; received in revised form 21 December 2001; accepted 6 January 2002

Abstract

$Al_2O_3/ZrO_2/Ag$ composites were obtained by intense attrition milling of silver and alumina powders with TZP balls. The characteristics of mixtures and the mechanical properties of sintered samples were investigated. Milling in acetone for 7 h results in a homogeneous submicron mixture. Ag composites (10 vol.%) CIPed at 300 MPa contain 8.1 vol.% tetragonal zirconia and 8.0 vol.% silver after sintering in air for 2 h at 1550 °C. Fracture toughness and bending strength as high as 5.44 MPa m and 586 MPa were obtained (645 MPa by post-HIPing). The incorporation of more silver (20 vol.%) is detrimental to microstructure quality and strength, but fracture toughness remains high thanks to crack bridging effects developed by ductile metallic inclusions. © 2002 Elsevier Science Ltd. All rights reserved.

Keywords: Ag; Al_2O_3–ZrO_2–Ag; Composites; Mechanical properties; Toughness

1. Introduction

Toughening brittle ceramics is a major research objective. One way is to incorporate second-phase inclusions which hinder the propagation of cracks, e.g. ductile metallic particles (Ni,[1] Fe[2]) are successful in toughening alumina. Silver is also of interest because of its transport properties, for instance in superconducting $Ag–YBa_2Cu_3O_{7-x}$[3] or in $Pb(Zr,Ti)O_3$ ferroelectrics where Ag dispersions result in an enhancement of the dielectric constant.[4] Most of the silver-ceramic systems can be fabricated through normal sintering in air, since silver is stable in air above 200 °C.[5]

Tuan et al. have shown that silver inclusions improve the mechanical[6] and transport[7] properties of alumina. At room temperature in air, flexural strength, fracture toughness, electrical resistivity, thermal diffusivity and electrical conductivity reach the following values when the silver content is 10 vol.%: 394 MPa, 4.7 MPa $m^{1/2}$, 11×10^{13} Ω cm, 14.7 $mm^2\ s^{-1}$, and 40 W $m^{-1}\ K^{-1}$ (compared to 325 MPa, 4.0 MPa $m^{1/2}$, 1.8×10^{13} Ω cm, 11.3 $mm^2\ s^{-1}$, and 32 W $m^{-1}\ K^{-1}$ for pure alumina). Moreover, it was shown that these composites have an interfacial thermal conductance of 4.1×10^8 W $m^{-2}\ K^{-1}$.

It has been shown[8] that the fracture resistance of Al_2O_3–Ag is increased by adding zirconia. In comparison to undoped alumina with similar density, the decrease in matrix grain size was significant (from 11.0 to 2.8 μm). The size of the silver inclusions was 2.2 μm. The flexural strength and toughness were increased from 390 to 630 MPa and from 4.6 to 6.6 MPa $m^{1/2}$, respectively. Intense attrition milling of alumina and silver powders with TZP balls is a way to get a fine homogeneous mixture with tetragonal zirconia dispersions. We have studied the influence of the type of alumina powder, the milling medium, and the silver content, on the characteristics of the mixtures and of the sintered bodies.

2. Experimental procedures

Alumina ((a) CL 3000, 99.8%, 2–3 μm, 0.45–0.65 $m^2\ g^{-1}$, Alcoa Chemie GmbH, Germany, and (b) TM-DAR, 99.99%, 0.2 μm, 14 $m^2\ g^{-1}$, Taimei Chemical Co. Ltd., Tokyo, Japan) and silver (Alfa, 99.9%, 1–3 μm, 0.5–1 $m^2\ g^{-1}$, Johnson Matthey Co., Danvers, USA) were attrition milled for 5 or 7 h in acetone with tetra-

* Corresponding author.
E-mail address: jerome.lalande@espci.fr (J. Lalande).
[1] Present address: Laboratoire Céramiques et Matériaux Minéraux, Ecole Supérieure de Physique et de Chimie Industrielles, 10 rue Vauquelin, 75005 Paris, France.

0955-2219/02/$ - see front matter © 2002 Elsevier Science Ltd. All rights reserved.
PII: S0955-2219(02)00031-6

gonal zirconia balls (3Y-TZP, diameter of 3 mm, Tosoh, Japan). The following notations were used to characterize the powders and samples: $^{(A)}$A for Alcoa alumina, $^{(T)}$A for Taimei alumina, Z for zirconia, $S_{10(20)}$ for 10 (20) vol.% silver, −5 (−7) for 5 (7) h milling time, and w as suffix for the mixture milled for 7 h in water instead of acetone. The slurry was dried for 1 day. The dried powder was sieved through a 200 μm mesh screen. A laser particle size analyser (Mastersizer S 2.15, Malvern Instruments) was used to measure the particle size distribution of the powders after milling. Data were obtained using the Fraunhofer model, which does not imply any value of refractive index. Pellets (1 cm in diameter and 5.3–5.5 cm in height) used for preliminary study of the sintering behavior of 10 vol.% Ag mixtures were shaped by uniaxial pressing at 50 MPa followed by cold isostatic pressing (CIP) at 100 to 900 MPa. The relative densities were determined based on theoretical densities of 3.97, 6.10, and 10.50 g cm^{-3} for Al_2O_3, t-ZrO_2 and Ag, respectively. The sintering was performed in air in a box furnace at temperatures between 1300 and 1600 °C for 1 or 2 h. The heating and cooling rates were 5 and 10 °C min^{-1}, respectively. The compacts were placed on alumina powder in plate-covered crucibles. $^{(A)}AZS_{20}$-7 samples were not covered so as to avoid silver droplets remaining on their surfaces. Hot isostatic pressing was performed after sintering on four 600 MPa-CIPed $^{(A)}AZS_{10}$-7 bars. Samples were heated at 15° min^{-1} under vacuum up to 500 °C, then under Ar pressure of 100 MPa up to 1000 °C, and further under 200 MPa up to 1500 °C and held for 20min, then samples were furnace cooled.

The final density was determined by Archimedes method in water. Since the partial pressure of silver is high at elevated temperature (10 mm Hg at 1575 °C),[5] the volume fraction of silver decreased during sintering and a silver-free surface layer was formed. The zirconia content in $^{(A)}$AZ-7 and $^{(A)}AZS_{10}$-7 (where the ratio silver fraction/alumina fraction is known) was determined from He pycnometry of the powder after drying at 400 °C for 3 h. The silver loss during sintering of pellets CIPed at 300 MPa was determined from the weight change. Phases in machined samples were analyzed by X-ray diffraction with Cu-K_α radiation. The ratio between the estimated phase contents in sintered $^{(A)}AZS_{10}$-7 and the area of not-superimposed diffraction peaks of the various phases were used to calculate the relative contents of zirconia and silver in samples. Some specimens sintered at 1550 °C for 2 h were polished then thermally etched at 1450 °C for 15 min to reveal the grain boundaries. The microstructure was examined by scanning electron microscopy.

Bars (2.7×3.8×36 mm^3) were prepared for mechanical testing. The samples were ground longitudinally to remove the silver-free layer and get parallel faces then polished with 15 to 3 μm diamond paste. Hardness was measured with a Vickers diamond indenter at 100 N. The tensile surface of six specimens was chamfered before determining strength by 4-point-bending at a loading rate of 0.5 mm min^{-1}.[9] The upper and lower spans were 12 and 24 mm, respectively. The fracture toughness of samples (2.7×5.8×36 mm^3) was determined by the single-edge-notched-beam (SENB) technique.[10] The notch was cut using a 250 μm-thick diamond saw and pre-cracked with a razor blade and 6 to 1 μm diamond paste. Friction-and-wear tests were performed at 24 °C at various degrees of moisture on polished surfaces of $^{(A)}AZS_{10}$-5 and $^{(T)}AZS_{10}$-5 samples. Test parameters were: 10 mm Al_2O_3 balls, under a 10 N normal load (F_n), along $\Delta x = 0.2$ mm for $n = 10^5$ times, at a frequency of 10 Hz. The friction and wear coefficients ($k = W_V/F_n \times s$, where s = 2 $\Delta x \times n$ and W_V is the wear volume measured at the optical microscope) were determined.

3. Results and discussion

3.1. Grain size after milling

The particle size distribution of the mixtures milled in acetone as function of silver content is shown in Fig. 1. Whereas the minimum particle size remains constant at about 0.2 μm, the distribution broadens with increasing

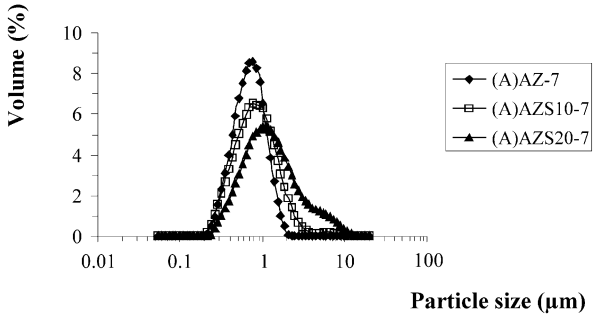

Fig. 1. Particle size distribution of 0, 10, and 20 vol.% Ag–Al_2O_3 mixtures milled in acetone for 7 h.

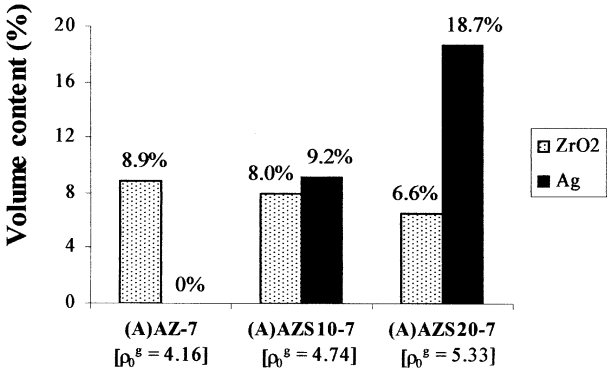

Fig. 2. Estimated composition and theoretical density ρ_0^g (g cm^{-3}) of green bodies.

silver content due to reduced attrition efficiency and possibly cold welding of the soft metal. As a result, the amount of zirconia incorporated during milling decreases with increasing silver content (Figs. 2 and 3). A 10 vol.% Ag mixture milled in water is slightly coarser: the median diameter is 0.85 μm compared to 0.78 μm when acetone is used. Besides, the zirconia content is estimated to 7.6% instead of 8.0%. The use of such a solvent seems to be responsible for slightly less mechanical wear and dispersion of the silver agglomerates. $^{(A)}AZS_{10}$-7w has similar green and sintered densities as $^{(A)}AZS_{10}$-7. Density and strength are slightly lower (Table 1).

3.2. Thermal behavior

The weight loss (−2.82%) during sintering (at 1550 °C for 2 h) of 300 MPa-CIPed $^{(A)}AZS_{10}$-7 bars was used to calculate their final silver content and set parameters for X-ray quantification. There is good agreement between calculations made from pycnometry and XRD. For $^{(A)}AZ$-7 for instance, the ratios between the zirconia and the alumina volume fractions are 0.095 and 0.097, respectively. The silver loss of $^{(A)}AZS_{10}$-7 samples is slightly decreased at increased CIP pressure (Fig. 3). Porosity probably closes at a lower sintering temperature when the green density is higher. As for 20 vol.% Ag mixtures, high weight loss, increasing with CIP pressure because more silver exsudates, is measured

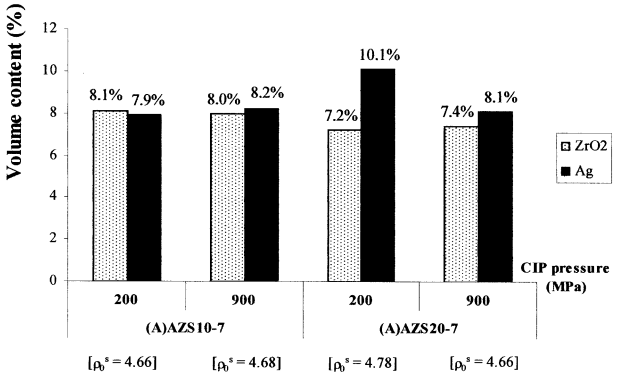

Fig. 3. Estimated composition and theoretical density ρ_0^s (g cm^{-3}) of sintered bodies.

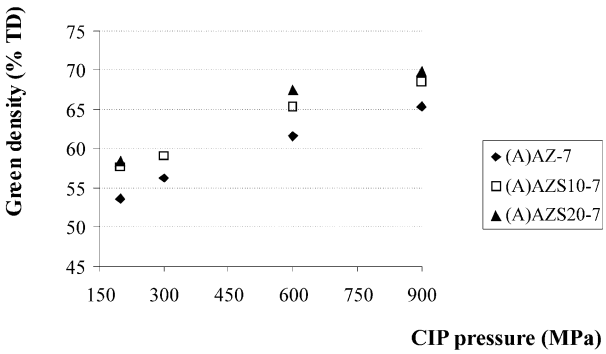

Fig. 4. Relative green density versus compacting pressure.

(−15.84% at 200 MPa, −20.04% at 900 MPa). The crucible containing $^{(A)}AZS_{20}$-7 samples must not be covered so as to avoid silver droplets remaining on their surfaces. Green and sintered density as function of CIP pressure are given in Fig. 4 and Table 1. Green density increases with silver content, due to plastic deformation. High densification is observed when sintering is performed at 1550 °C for 2 h.

3.3. Microstructures

As also shown by Tuan et al.,[8] nearly equiaxed silver inclusions (bright color in Fig. 5) distribute randomly

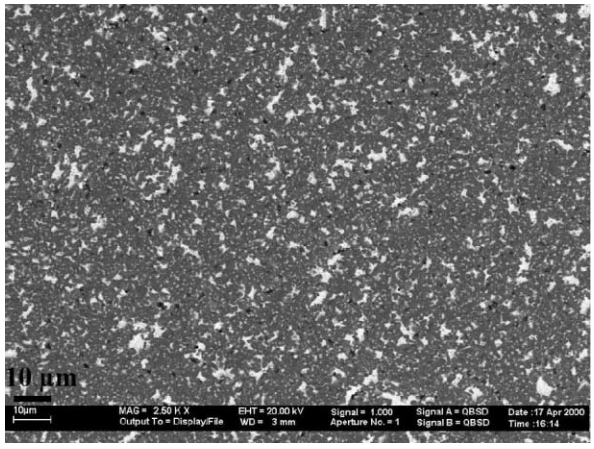

Fig. 5. $^{(A)}AZS_{10}$-7 CIPed at 300 MPa and sintered at 1550 °C for 2 h.

Table 1
Mechanical properties of samples CIPed at 600 MPa and sintered at 1550 °C for 2 h

	Density after sintering (% TD)	Density after grinding (% TD)	Ag volume content (%)	Vickers hardness (GPa)	Bend strength (MPa)	Fracture toughness (MPa$\sqrt{m}$)
$^{(A)}AZ$-7	97.8	98.1	0	18.1±0.9	595±42	4.58±0.21
$^{(A)}AZS_{10}$-7	96.8	98.5	8.1	13.7±0.8	587±59	5.09±0.21
$^{(A)}AZS_{20}$-7	98.5	98.5	8.8	11.2±0.5	396±25	5.41±0.23
Post-HIPed $^{(A)}AZS_{10}$-7	97.4	98.7	8.1	12.6±0.3	645±49	–
$^{(A)}AZS_{10}$-7w	97.6	98.7	7.0	13.9±1.1	514±66	–

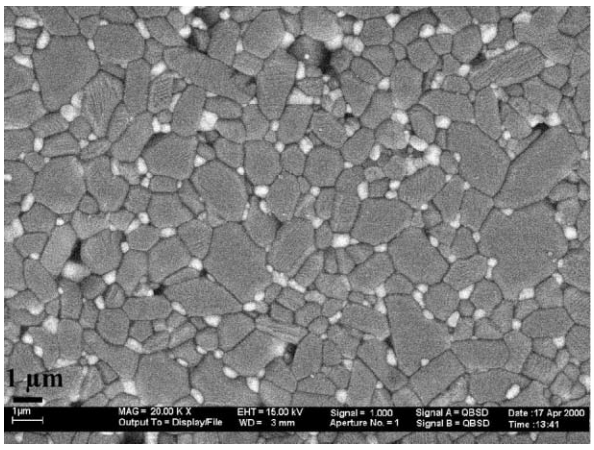

Fig. 6. $^{(A)}$AZ-7 CIPed at 300 MPa and sintered at 1550 °C for 2 h (thermally etched at 1450 °C).

throughout the Al_2O_3 matrix rather than forming thin elongated metal foils. Their size lies between 0.5 and 4 µm. A silver-free surface layer is formed during thermal etching leading to holes in places where silver was located. $^{(A)}$AZ-7 samples are well densified (Fig. 6). Al_2O_3 grains are approximately 0.2 to 3 µm. ZrO_2 particles (~0.1–0.5 µm) are located at multiple grain junctions.

3.4. Mechanical properties

Density, hardness, and bending strength of $^{(A)}$AZ-7 vary in the range 4.05–4.08, 17.1–8.0 GPa and 540–595 MPa, respectively (Fig. 7 and 8). These values are typical for ZrO_2-reinforced Al_2O_3. The hardness of $^{(A)}AZS_{10}$-7 increases with density to reach a maximum for materials CIPed at 600 MPa (Fig. 7). The hardness of sintered $^{(A)}AZS_{20}$-7 depends on CIP pressure (Fig. 7: 11.8±0.3 GPa at 900 MPa and 9.8±0.7 GPa at 200 MPa), which underlines the decrease in hardness with increasing silver content. The latter contains 2% more

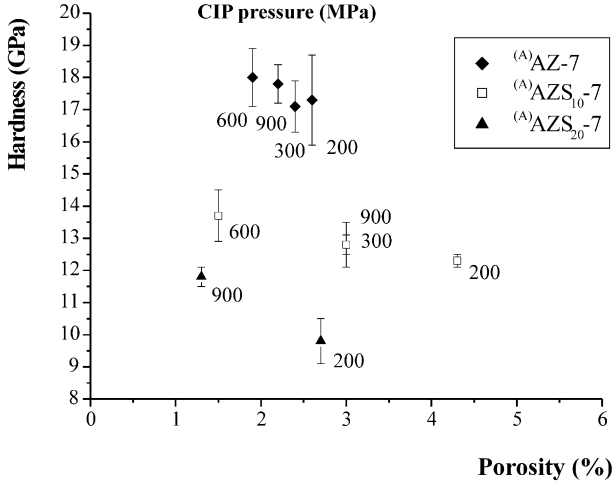

Fig. 7. Hardness versus porosity.

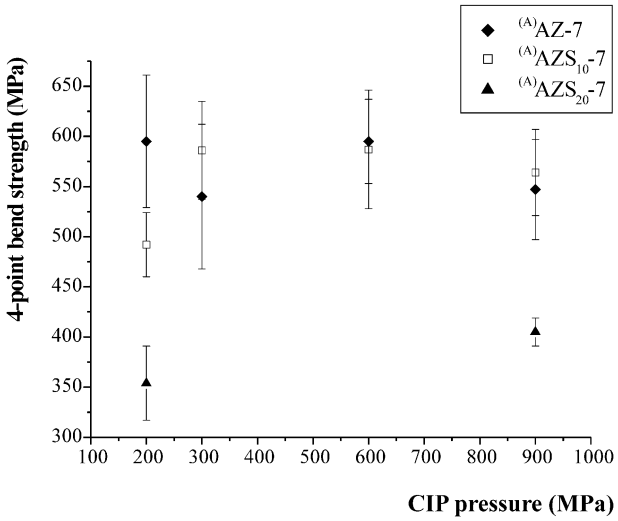

Fig. 8. Four-point bend strength versus CIP pressure.

silver, soft element (Fig. 3). In Ni-containing alumina ceramics,[1] increasing amount of ductile inclusions seems to reduce the sensitivity of hardness to porosity. This has also been emphasized for $YBa_2Cu_3O_{7-x}$/Ag composites.[3]

The bend strength of $^{(A)}AZS_{10}$-7 samples CIPed at 300 and 600 MPa is ~590 MPa (Fig. 8). When these samples are post-HIPed, the density ($\rho = 4.61$ g cm^{-3}) is only slightly increased, but the strength is increased to 645±49 MPa. The good strength of $^{(A)}$AZ-7 and $^{(A)}AZS_{10}$-7 is attributable to matrix grain refinement. Since the thermal expansion coefficient of silver (22×10^{-6} K^{-1}) is higher than that of alumina (8.8×10^{-6} K^{-1}), thermal mismatch stress may cause cavity formation and interfacial debonding during cooling. Liu and al.[7] estimated the critical silver inclusion size above which circumferential cracks are generated. The large (>2.7 µm) silver inclusions and defects observed in $^{(A)}AZS_{20}$-7 microstructures are clearly responsible for

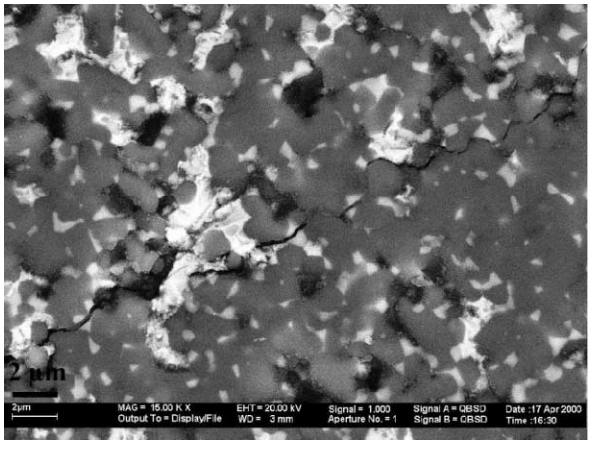

Fig. 9. Crack bridging in $^{(A)}AZS_{10}$-7 CIPed at 300 MPa and sintered at 1550 °C for 2 h.

strengths as low as 400 MPa. Tuan et al.[8] obtained 10 vol.% Ag–Al_2O_3 composites from tumble milled Taimei Al_2O_3–Ag_2O powder with only 1.2% porosity, strength of 490 MPa, and toughness of 5.3 MPa $m^{1/2}$. These values which are higher than those they obtained with another alumina powder[6] can be attributed to the smaller inclusion size (1.4 μm instead of 2.5 μm), since the matrix grain size is similar (4.1 μm instead of 4.2 μm).

Tetragonal zirconia is known to undergo a martensitic transformation. The expansion of thermally transformed particles results in stress-induced microcracking ahead of a propagating crack, thereby dissipating energy.[11] Indentation crack lengths were in the range 365–380 μm for $^{(A)}$AZ-7, 255–275 μm for $^{(A)}AZS_{10}$-7, and 215–250 μm for $^{(A)}AZS_{20}$-7 which agrees with the fracture toughness that increases with silver content (Table 1). As the zirconia content does not vary much in the materials studied, it is clear that the silver inclusions are effective in toughening via crack bridging, thanks to their plastic behavior (Fig. 9). High fracture toughness was achieved with $^{(A)}AZS_{20}$-7 CIPed at 600 MPa as well as with AZS_{10}-7 CIPed at 300 MPa (5.44 ± 0.52 MPa $m^{1/2}$, $\rho = 4.50$ g cm^{-3}). $^{(A)}AZS_{20}$-7 has a high fracture toughness despite a low strength. It was also measured for 20 vol.% Ag–$YBa_2Cu_3O_{7-x}$ (2.5 times that of the plain ceramic in spite of 2.2% more porosity).[3]

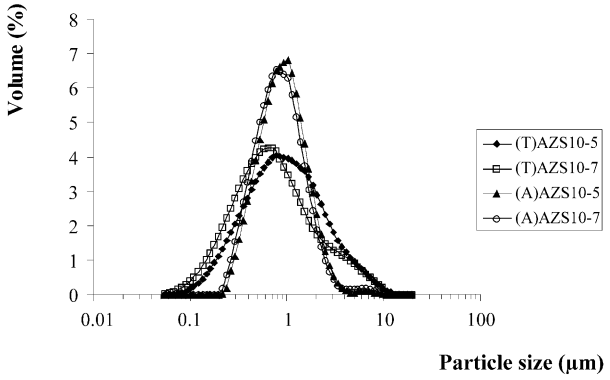

Fig. 10. Particle size distribution of the 10 vol.% Ag–Al_2O_3 mixtures milled in acetone.

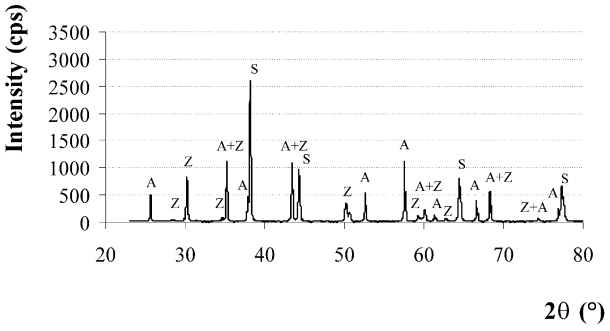

Fig. 11. XRD diagram of the polished surface of a 300 MPa-CIPed and sintered $^{(A)}AZS_{10}$-7 pellet. A: α-Al_2O_3; Z: Tetragonal ZrO_2; S: Silver.

3.5. Influence of milling time and composition on attrition efficiency

Powders are refined in such a way that all median diameters are under 0.8 μm after 7 h of attrition, whatever the alumina size (Fig. 10). However, the particle size distribution is broader with Taimei Al_2O_3. It starts at 40 nm, which agrees with the finer characteristics of the raw powder, and $\phi_{90\%} = 2.81$ μm instead of 1.67 μm with Alcoa Al_2O_3. A second mode is visible with $^{(T)}AZS_{10}$-7. According to Table 2, mixtures milled for a shorter time (5 h) contain less zirconia, as when Taimei is used instead of Alcoa alumina (compare Fig. 12 with Fig. 11), due to less mechanical wear. Moreover, $^{(T)}AZS_{10}$ bodies lose slightly less silver during sintering (−2.06% and −1.95% for $^{(T)}AZS_{10}$-7 CIPed at 300 and 600 MPa, respectively).

Taimei alumina leads to lower green densities (Fig. 13) which may be due to the higher fraction of ultrafine particles. However, they activate densification. For 250 MPa-CIPed samples for instance, the density after sintering at 1350 °C for 1 h is 3.11 g cm^{-3} for $^{(A)}AZS_{10}$-5 and 3.42 g cm^{-3} for $^{(T)}AZS_{10}$-5 (Fig. 14). But high densification ($\rho = 4.55$ g cm^{-3}) is observed for both kinds of mixtures when sintering is performed at 1600 °C for 1 h. Densities of $^{(A)}AZS_{10}$-5 CIPed at 200 and 300 MPa then sintered at 1550 °C for 2 h are 4.46 g cm^{-3} and 4.51 g cm^{-3}, respectively.

The grain size distribution of the matrix after sintering is correlated to that after milling (Figs. 15 and 16). There are some larger matrix grains when Taimei alumina is used. More grain growth could also be

Table 2
Estimated composition and theoretical density of green and sintered bodies CIPed at 300 MPa

	$^{(A)}AZS_{10}$-5		$^{(T)}AZS_{10}$-5		$^{(T)}AZS_{10}$-7	
	Green	Sintered	Green	Sintered	Green	Sintered
ZrO_2 volume content	6.3%	6.5%	4.3%	4.4%	5.5%	5.6%
Ag volume content	9.4%	7.0%	9.6%	8.4%	9.4%	7.7%
Theoretical density (g cm^{-3})	4.72	4.57	4.69	4.61	4.70	4.58

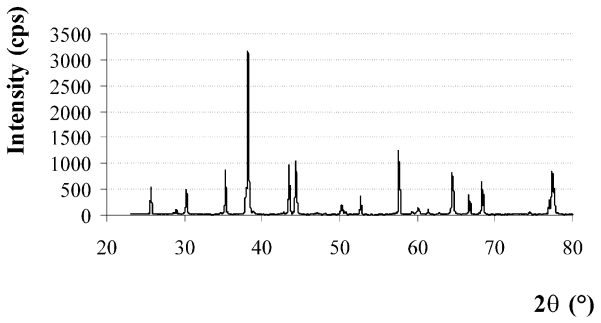

Fig. 12. XRD diagram of the polished surface of a 300 MPa-CIPed and sintered $^{(T)}AZS_{10}$-7 pellet.

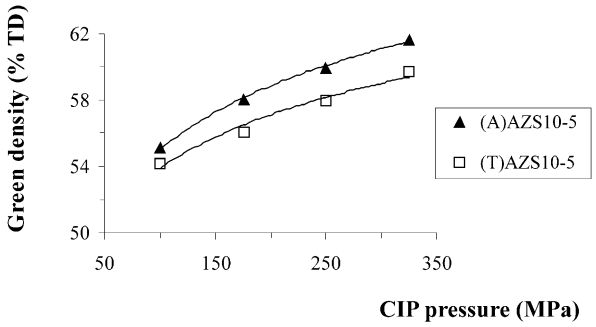

Fig. 13. Relative density of green AZS_{10}-5 bodies.

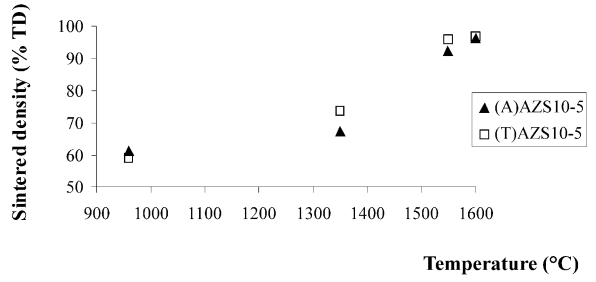

Fig. 14. Relative density of AZS_{10}-5 samples CIPed at 300 MPa and sintered at various temperatures for 1 h.

responsible for this feature, because this kind of mixture densifies faster, hence the grain boundary motion develops more easily. $^{(A)}AZS_{10}$-5 samples contain more zirconia, the grains of which are larger and only located at grain boundaries, unlike $^{(T)}AZS_{10}$-5 samples where many ZrO_2 grains are trapped in alumina grains.

For a same density, $^{(A)}AZS_{10}$-5 sintered bodies CIPed at 175 MPa have a bending strength (471±41 MPa) which is 21% higher than that of $^{(T)}AZS_{10}$-5 (389±38 MPa) CIPed at 325 MPa, which suggests that a high fraction of particles in the micron size range is detrimental to fracture strength. The lower hardness of $^{(T)}AZS_{10}$-5 (13.4±0.4 GPa compared to 14.1±0.3 GPa for $^{(A)}AZS_{10}$-5) may be due to the presence of large alumina grains.

Friction and wear tests were performed on the densest $^{(A)}AZS_{10}$-5 and $^{(T)}AZS_{10}$-5 sintered bodies. These tests

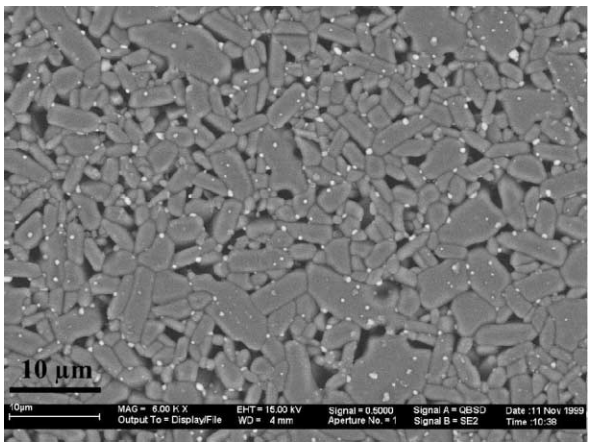

Fig. 15. $^{(T)}AZS_{10}$-5 CIPed at 325 MPa and sintered at 1600 °C for 1 h (thermally etched at 1450 °C).

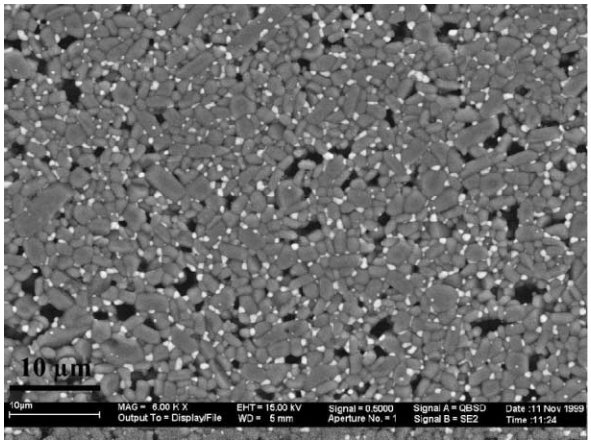

Fig. 16. $^{(A)}AZS_{10}$-5 CIPed at 175 MPa and sintered at 1600 °C for 1 h (thermally etched at 1450 °C).

show that additions of silver to alumina result in a decrease in wear of the sliding alumina ball as well as of the whole system, which suggests the possible use of this material for tribological applications, and an increase of the friction coefficient (Table 3), which is however less than 0.56 measured in air at room temperature for zirconia-toughened alumina on alumina, with a spherically ended pin on flat disk test geometry.[12] Our results also show a decrease in friction coefficient with increasing humidity for all investigated materials. Further study is necessary to explain the influence of silver and atmosphere.

The Alcoa powder is cheaper than Taimei, but higher bending strengths are obtained with $^{(T)}AZS_{10}$-7 CIPed at low pressure (Table 4) or sintered at 1550 °C only for 1 h ($\sigma_b = 575 \pm 65$ MPa, $\rho = 4.53$, $H_V = 12.0 \pm 0.2$ GPa). When too high compacting pressures or sintering times are used, the samples are likely to experience grain growth without further densification, which is detrimental to mechanical strength.

Table 3
Wear, k, and friction, f, coefficients in various atmospheres

Material	Relative humidity (%)	k ($\times 10^{-6}$ mm^3.N^{-1}.m^{-1})			f
		Ball	Material surface	Sum	
Al_2O_3 *(TKRD0187)*	1	0.13	0.01	0.14	0.33
	52	0.09	0.03	0.12	0.27
	100	0.13	0.04	0.17	0.25
$^{(T)}AZS_{10}$-5	2	0.04	0.03	0.06	0.42
	47	0.02	0.03	0.05	0.36
	100	0.03	0.03	0.07	0.33
$^{(A)}AZS_{10}$-5	2	0.03	0.04	0.07	0.52
	48	0.02	0.04	0.05	0.40
	100	0.02	0.06	0.08	0.35

Table 4
Mechanical properties of $^{(T)}AZS_{10}$-7 bodies sintered at 1550 °C for 2 h

CIP pressure (MPa)	Density after compaction (g cm^{-3})	Density after sintering (g cm^{-3})	Density after grinding (g cm^{-3})	Vickers hardness (GPa)	Bend strength (MPa)
200	2.60	4.48	4.52	13.1±0.2	560±86
300	2.78	4.51	4.55	13.0±0.4	546±72
600	3.00	4.49	4.53	–	533±96

4. Conclusions

1. Attrition milling of alumina and silver in acetone leads to slightly finer and more homogeneous Ag distribution in the alumina matrix than when water is used.
2. An ultrafine alumina powder is detrimental for refining the mixture.
3. The strength of a 10 vol.% Ag material is 590 MPa, similar to that of the corresponding ZrO_2–Al_2O_3 ceramic, and fracture toughness is higher: 5.1 MPa m$^{1/2}$ compared to 4.6 MPa m$^{1/2}$ without silver addition.
4. It is not possible to get interconnected metal inclusions with this system because silver vaporizes during sintering. High amounts of silver degrade the mechanical resistance. However, the toughness enhancement achieved by crack bridging is still observed by incorporating 20 vol.% silver.

Acknowledgements

The authors gratefully acknowledge Professor P. Boch (Laboratoire Céramiques et Matériaux Minéraux, ESPCI, Paris, France) for his commitment and Dr. D. Klaffke (MFG, BAM, Berlin, Germany) for performing wear and friction tests.

References

1. Tuan, W. H. and Brook, R. J., The toughening of alumina with nickel inclusions. *J. Eur. Ceram. Soc.*, 1990, **6**, 31–37.
2. Trusty, P. A. and Yeomans, J. A., The toughening of aluminia with iron: effects of iron distribution on fracture toughness. *J. Eur. Ceram. Soc.*, 1997, **17**(4), 495–504.
3. Tuan, W. H. and Wu, J. M., Effect of microstructure on the hardness and fracture toughness of $YBa_2Cu_3O_{7-x}$/Ag composites. *J. Mater. Sci.*, 1993, **28**, 1415–1420.
4. Hwang, H. J., Yasuoka, M., Sando, M., Toriyama, M. and Niihara, K., Fabrication, Sinterability, and Mechanical Properties of Lead Zirconate Titanate/Silver Composites. *J. Am. Ceram. Soc.*, 1999, **82**(9), 2417–2422.
5. Weast, R. C., *Handbook of Chemistry and Physics*, CRC Press Inc., 1978–1979, 59th Edn, D-239.
6. Tuan, W. H. and Chou, W. B., The corrosion behaviour of Al_2O_3 toughened by Ag particles. *J. Eur. Ceram. Soc.*, 1996, **16**, 583–586.
7. Liu, D. M. and Tuan, W. H., Microstructure and thermal conduction properties of Al_2O_3-Ag composites. *Acta Mater.*, 1996, **44**(2), 813–818.
8. Tuan, W. H. and Chen, W. R., Mechanical properties of alumina-zirconia-silver composites. *J. Am. Ceram. Soc.*, 1995, **78**(2), 465–469.
9. ASTM Standard C1161–94, Standard Test Method for Flexural Strength of Advanced Ceramics at Ambient Temperature. *Annual Book of ASTM Standards*, General Products, Chemical Specialties, and End Use Products, Vol. 15.01 Refractories; Carbon & Graphite Products; Activated Carbon; Advanced Ceramics, ASTM, PA, 1997, pp. 309–315.
10. ASTM Standard E399–707, Standard Test Method for Plane-Strain Fracture Toughness of Metallic Materials. *Annual Book of ASTM Standards*, Vol. 03.01, Metals Tests Methods and Analytical Procedures. 1997, pp. 408–438.
11. Claussen, N., Fracture Toughness of Al_2O_3 with an Unstabilized ZrO_2 Dispersed Phase. *J. Am. Ceram. Soc.*, 1976, **59**(1–2), 49–51.
12. Blau, P. J., *ASM Handbook, Vol. 18: Friction, Lubrication, and Wear Technology*, ASM International.